Automatic balancing of a rigid rotor with misaligned shaft

D.J. Rodrigues[1,a], A.R. Champneys[1,b], M.I. Friswell[2,c], R.E. Wilson[1,d]

[1]Department of Engineering Mathematics, University of Bristol, Queens Building, University Walk, Bristol BS8 1TR
[2]Department of Aerospace Engineering, University of Bristol, Queens Building, University Walk, Bristol BS8 1TR

[a]D.J.Rodrigues@bristol.ac.uk, [b]A.R.Champneys@bristol.ac.uk, [c]M.I.Friswell@bristol.ac.uk, [d]Re.Wilson@bristol.ac.uk.

Keywords: Automatic balancing, Euler angles, Rigid rotor, Shaft misalignment.

Abstract. We present a nonlinear analysis of the dynamics of an automatic ball balancer (ABB) for rotors which are both eccentric and misaligned. The ABB consists of two or more ball bearings which are free to travel around a circular race at a fixed distance from the shaft. The balls, after a transient response, find a steady state which balances the rotor. Following the previous work of Green *et al*. at Bristol, we have included the effect of shaft misalignment which causes the rotor to precess. This can be countered by having two ABB races at different axial locations along the shaft. Mathematically, we use a Lagrangian approach to derive the equations of motion for the system. It is found that, contrary to the case of flexible rotors that are subject to eccentricity and shaft bending, there is no choice of co-ordinate system which leads to autonomous governing equations. Simulations are then computed which illustrate the role of the ball damping coefficient.

Introduction

One of the primary causes of vibration in rotating machinery is mass imbalance, this occurs when the principal axis of the moment of inertia is not coincident with the axis of rotation. For a rigid rotor the imbalance is usually eliminated by adding (or subtracting) correction masses in two distinct planes in such a way as to realign and recentre the principal axis. However when using this method, the rotor has to be rebalanced every time its mass distribution changes. This limitation motivates the study of self-compensating balancing devices, in which masses automatically redistribute themselves so as to eliminate any imbalance.

One such device is the automatic ball balancer (ABB), which consists of a series of balls that are free to travel, around a race filled with viscous fluid. This idea was initially proposed in 1904 [1], and since then ABB's have been incorporated into many products including optical disc drives, machine tools and washing machines. The first study of an ABB was carried out by Thearle in 1932 [2], who demonstrated the existence of a stable steady state at rotation speeds above the first critical frequency. More recently, Chung *et al.* [3] have studied the stability of automatic balancing for an eccentric flexible rotor, Chao *et al.* [4] have looked at the non-planar effects of an optical disk drive fitted with an ABB and Green *et al.* [5] have focused on using numerical continuation to map the bifurcations between different attracting states in a Jefcott rotor fitted with an ABB.

The rest of this paper is outlined as follows. In Section 2 we present a fully geometric model for two-plane automatic balancing of a rigid rotor [6]. Our techniques are fully nonlinear and do not rely on small angle or constant spin speed assumptions, and so may be applicable to many other fields, such as celestial mechanics and the dynamics of spinning spacecraft [7]. In Section 3 we focus on the two-plane autobalancing of a rotor with shaft misalignment and simulate responses for different values of the ball damping parameter. Finally, in Section 4 we draw conclusions and discuss how we would make the system amenable to bifurcation analysis.

Two-plane automatic balancing

Reference frames and generalized co-ordinates. In describing the dynamics of a rigid body it is useful to consider the relation between an xyz frame fixed to the body and an inertial XYZ space frame, see Figure 1. Firstly a translation is needed to place the XYZ axes onto the $X'Y'Z'$ axes which is parallel to XYZ but with the same origin as the xyz body axes. Then the orientation of the xyz body axes, relative to the $X'Y'Z'$ frame, can be specified through the use of Euler angles where we will use the convention set out below.

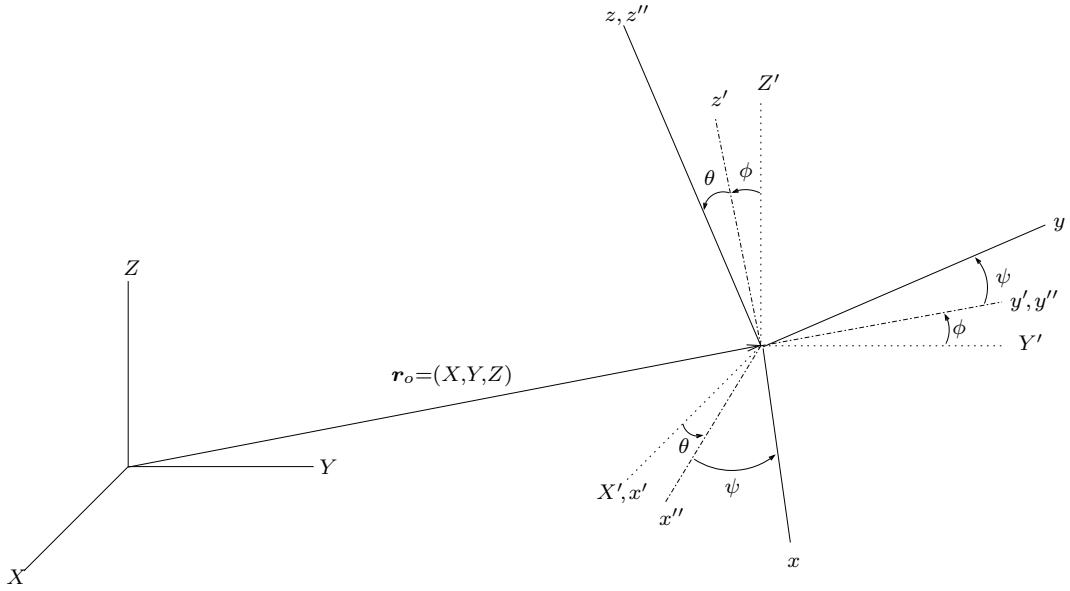

Fig. 1: Definition of co-ordinate system.

Here, a rotation by an angle ϕ about the X' axis results in the primed co-ordinate system $x'y'z'$. This intermediate sytem is then rotated by an angle θ about the y' axis resulting in the double primed system $x''y''z''$. Finally, a rotation ψ about the z'' axis gives the unprimed xyz co-ordinate system. The full rotation R can be concisely written in matrix form as

$$\mathsf{R} = \mathsf{R}_\psi \mathsf{R}_\theta \mathsf{R}_\phi, \tag{1}$$

where

$$\mathsf{R}_\phi = \begin{bmatrix} 1 & 0 & 0 \\ 0 & \cos\phi & \sin\phi \\ 0 & -\sin\phi & \cos\phi \end{bmatrix}, \quad \mathsf{R}_\theta = \begin{bmatrix} \cos\theta & 0 & -\sin\theta \\ 0 & 1 & 0 \\ \sin\theta & 0 & \cos\theta \end{bmatrix}, \quad \mathsf{R}_\psi = \begin{bmatrix} \cos\psi & \sin\psi & 0 \\ -\sin\psi & \cos\psi & 0 \\ 0 & 0 & 1 \end{bmatrix}. \tag{2}$$

The use of three separate axes eliminates any polar singularity, furthermore in the small angle limit, ϕ and θ reduce to projection angles, which are commonly seen in the rotordynamics literature [6]. Thus the full co-ordinate transformation from xyz to XYZ is given by

$$\boldsymbol{r}_{XYZ} = \boldsymbol{r}_o + \mathsf{R}^{\mathrm{T}} \boldsymbol{r}_{xyz}, \tag{3}$$

where $\boldsymbol{r}_{XYZ}$ and $\boldsymbol{r}_{xyz}$ are the position vectors in the XYZ and xyz systems respectively, and $\boldsymbol{r}_o = [X, Y, Z]$ is the position vector of the xyz systems origin. Thus the generlized co-ordinates $\boldsymbol{q} = [X, Y, Z, \phi, \theta, \psi]^{\mathrm{T}}$ can be used to describe the motion of any rigid body.

Model. The model shown in Figure 2 consists of a balanced rotor of mass M and moment of inertia $\mathsf{I} = \mathrm{diag}[I_x, I_y, I_z]$ with respect to the xyz axes. The mass imbalance is introduced through two point masses m_1, m_2, fixed to the rotor in planes z_1, z_2, with eccentricities ε_1, ε_2, and angular positions α_1, α_2 so that

both static and couple imbalance are present. This setup is dynamically equivalent to the most general rigid rotor, which has both an offset centre of mass and a misaligned principal axis. The autobalancing device has two races R_1 and R_2, each fitted with n balls, which are represented as points of mass m_i, in plane z_i, with eccentricity ε_i and angular position α_i, where $i = 3 \dots n+2$, and $i = n+3 \dots 2n+2$ correspond to the balls in R_1 and R_2 respectively. The supports S_1 and S_2, have rest positions $[0, 0, l_1]$ and $[0, 0, -l_2]$, with stiffness $\mathsf{K}_j = \text{diag}[k_{x_j}, k_{y_j}, k_{z_j}]$, and damping $\mathsf{C}_j = \text{diag}[c_{x_j}, c_{y_j}, c_{z_j}]$, $j = 1, 2$ with respect to the XYZ axes.

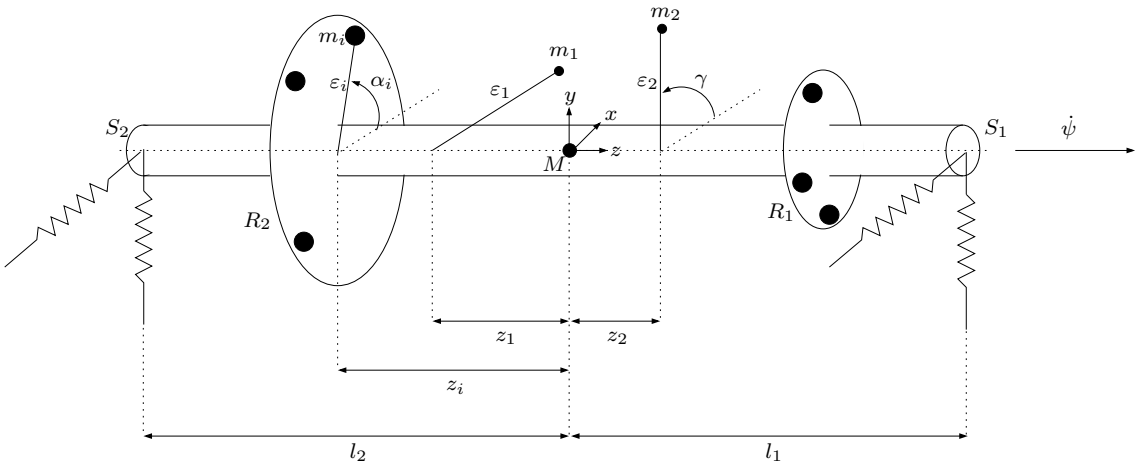

Fig. 2: Two-plane autobalancing rotor model.

Lagrangian formulation of the equations of motion. We begin by writing the position vectors of the centre of mass (COM), imbalances and balancing balls in the XYZ co-ordinate system. Using (3) we have

$$\boldsymbol{r}_M = \begin{bmatrix} X \\ Y \\ Z \end{bmatrix}, \qquad \boldsymbol{r}_{m_i} = \begin{bmatrix} X \\ Y \\ Z \end{bmatrix} + \mathsf{R}^{\mathrm{T}} \begin{bmatrix} \varepsilon_i \cos\alpha_i \\ \varepsilon_i \sin\alpha_i \\ z_i \end{bmatrix}, \; i = 1 \dots 2n+2. \tag{4}$$

Without loss of generality we can take $\alpha_1 = 0$ and $\alpha_2 = \gamma$ where γ is the constant phase between the two imbalances.

Next we write the angular velocity in the body axis, since it is in these axes in which the inertia matrix takes a diagonal form. As $\boldsymbol{\omega}_\phi$ is parallel to the space X axis, its components in the body axis are given by applying the complete rotation R. Now $\boldsymbol{\omega}_\theta$ lies along the intermediate y' axis and so we apply only the last rotation R_ψ, finally $\boldsymbol{\omega}_\psi$ lies along the body z axis and so needs no further work. Thus the components of $\boldsymbol{\omega}$ in the body axis are given by

$$\begin{aligned} \boldsymbol{\omega} &= \mathsf{R} \begin{bmatrix} \dot{\phi} \\ 0 \\ 0 \end{bmatrix} + \mathsf{R}_\psi \begin{bmatrix} 0 \\ \dot{\theta} \\ 0 \end{bmatrix} + \begin{bmatrix} 0 \\ 0 \\ \dot{\psi} \end{bmatrix}, \\ &= \begin{bmatrix} \dot{\phi}\cos\theta\cos\psi + \dot{\theta}\sin\psi \\ -\dot{\phi}\cos\theta\sin\psi + \dot{\theta}\cos\psi \\ \dot{\phi}\sin\theta + \dot{\psi} \end{bmatrix}. \end{aligned} \tag{5}$$

The kinetic energy $\mathcal{T}$ is now given by (see also the appendix)

$$\mathcal{T} = \frac{1}{2}\boldsymbol{\omega}^{\mathrm{T}}\mathsf{I}\boldsymbol{\omega} + \frac{1}{2}M\dot{\boldsymbol{r}}_M^2 + \frac{1}{2}\sum_{i=1}^{2n+2} m_i \dot{\boldsymbol{r}}_{m_i}^2. \tag{6}$$

The potential $\mathcal{V}$ comes from the elastic energy due to the deflection $\boldsymbol{r}_{S_1}$ and $\boldsymbol{r}_{S_2}$ of the supports S_1 and S_2 thus

$$\mathcal{V} = \frac{1}{2}\sum_{j=1}^{2} \boldsymbol{r}_{S_j}^{\mathrm{T}} \mathsf{K} \boldsymbol{r}_{S_j}, \tag{7}$$

where

$$\boldsymbol{r}_{S_j} = \left(\begin{bmatrix} X \\ Y \\ Z \end{bmatrix} + \mathsf{R}^{\mathrm{T}} \begin{bmatrix} 0 \\ 0 \\ \tilde{l}_j \end{bmatrix} \right) - \begin{bmatrix} 0 \\ 0 \\ \tilde{l}_j \end{bmatrix}, \qquad \tilde{l}_1 = l_1, \quad \tilde{l}_2 = -l_2. \tag{8}$$

Similarly Rayleigh's dissapation function $\mathcal{F}$ can be written as

$$\mathcal{F} = \frac{1}{2}\sum_{j=1}^{2} \dot{\boldsymbol{r}}_{S_j}^{\mathrm{T}} \mathsf{C} \dot{\boldsymbol{r}}_{S_j} + \frac{1}{2}\sum_{i=3}^{2n+2} c_b \dot{\alpha}_i, \tag{9}$$

where the ball damping coefficient c_b, arises from the drag on the balls as they pass through a viscous fluid in the race.

The equations of motion can now be generated by applying Lagrange's equations

$$\frac{\mathrm{d}}{\mathrm{d}t}\left(\frac{\partial \mathcal{L}}{\partial \dot{q}_k}\right) - \frac{\partial \mathcal{L}}{\partial q_k} = Q_k, \tag{10}$$

where $\mathcal{L} = \mathcal{T} - \mathcal{V}$ is the Lagrangian, and $\boldsymbol{q} = [X, Y, Z, \phi, \theta, \psi, \alpha_i]^{\mathrm{T}}$ $i = 3 \ldots 2n+2$, are the generalised co-ordinates. The generalised forces not arising from a potential Q_k, are given by $-\frac{\partial \mathcal{F}}{\partial \dot{q}_k}$ except in the equation for ψ where we must also add the driving torque $\tau(\dot{\psi})$.

Balancing of a misaligned rotor

Model parameters. We have used the computer algebra system `Maple` to derive the equations of motion (omitted here) from (10). The equations are then transfered without resorting to linearization into `Matlab` where they are solved numerically. The model rotor used for simulation has parameters $M = 1\,\mathrm{kg}$, $I_x = I_y = 1\,\mathrm{kg\,m^2}$, $I_z = 0.5\,\mathrm{kg\,m^2}$, $l_1 = l_2 = 0.5\,\mathrm{m}$. The COM is confined to the XY plane, and the spin speed $\dot{\psi} = \omega$, is assumed constant with $\omega = 40\,\mathrm{rad\,s^{-1}}$. Both supports are identical, with stiffness $\mathsf{K}_i = \mathrm{diag}[k, k, k]$, $k = 50\,\mathrm{N\,m^{-1}}$ and damping $\mathsf{C}_i = \mathrm{diag}[c, c, c]$, $c = 5\,\mathrm{N\,s\,m^{-1}}$.

The imbalance masses have values $m_1 = m_2 = 0.04\,\mathrm{kg}$, $e_1 = e_2 = 0.1\,\mathrm{m}$, $z_1 = -z_2 = 0.1\,\mathrm{m}$ and $\alpha_2 = \gamma = \pi$, which corresponds to a rotor whose imbalance occurs solely through misalignment. The ABB has parameters $m_i = 0.01\,\mathrm{kg}$, $e_i = 0.1\,\mathrm{m}$, $i = 3 \ldots 6$, $z_3 = z_4 = 0.25\,\mathrm{m}$, $z_5 = z_6 = -0.25\,\mathrm{m}$, corresponding to two races with two balls each. Finally the damping of the balls in the race c_b, is the parameter which is to be varied.

Simulations. Numerical simulations which illustrate the influence of the ball damping coefficient c_b, are shown in Figure 3. The top graphs show the vibration amplitude of the first support $A_1 = |\boldsymbol{r}_{S_1}|$, and the ball angles are shown underneath.

In the underdamped regime shown on the left, the balls initially oscillate about the unstable balanced positions, before destabilising completely at around $t = 50\,\mathrm{s}$. The resulting vibrations are an order of magnitude worse than the motion without the ABB. For high damping on the right, these oscillations are prevented, but the balls take a long time to reach the balanced state. Ideally we desire critical damping where the balls reach the equilibrium position in the minimum time without oscillation, as illustrated in the middle graphs.

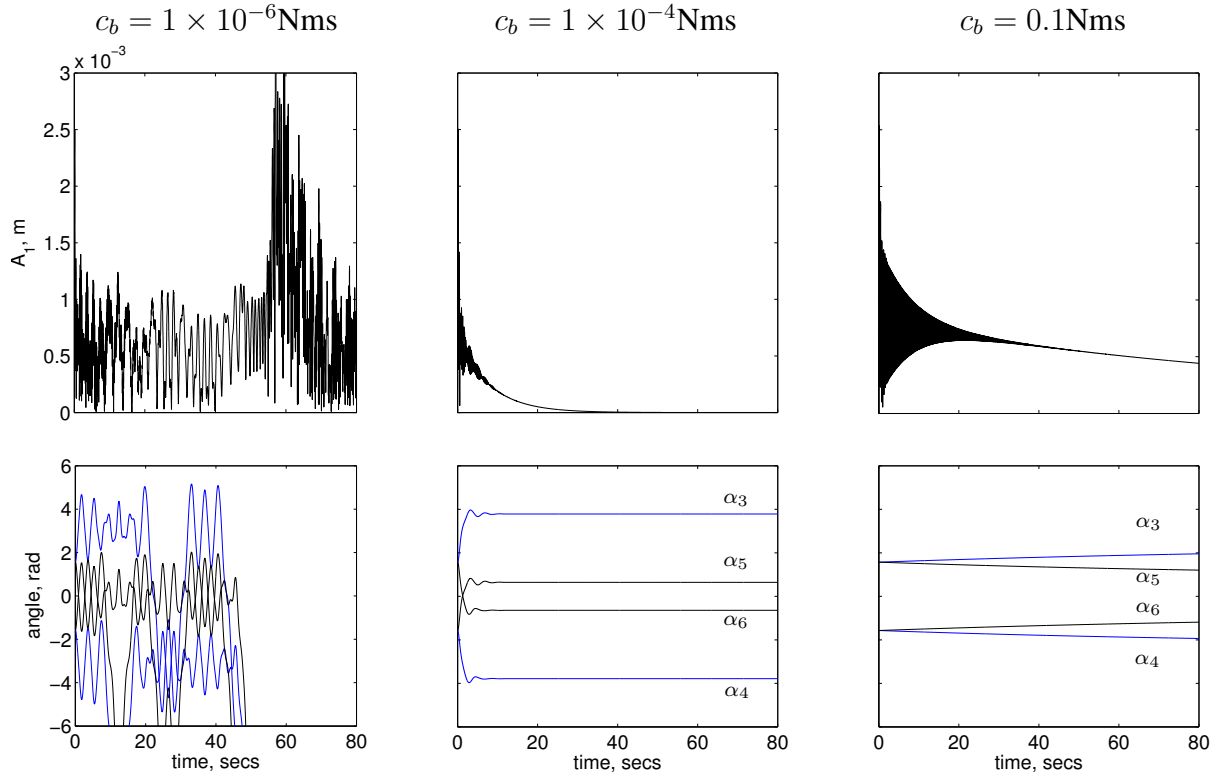

Fig. 3: Influence of ball damping c_b on the support vibrations and ball positions

Conclusion

We have presented a fully nonlinear geometric model for the two-plane balancing of a rigid rotor. In previous studies [3,5] of flexible and planar rotors, autonomous equations are derived by formulating the Lagrangian in the rotating frame. However, in the present case of a non-planar rigid rotor, the spin angle $\psi = \omega t$, is taken about a body z axis which is not parallel to the space Z axis. As a consequence, it is not possible to use the rotating frame to forge equations, which are both autonomous, and satisfy the condition that the rotor moves in the horizontal $Z = 0$ plane.

We have provided simulations for the two-plane automatic balancing of a misaligned rotor. It is shown that the two-race mechanism can eliminate not only vibrations due to radial motion, but also those due to angular displacement. However automatic balancing can only be achieved in regions of parameter space where the balanced state is stable, in particular an appropriate choice of the ball damping coefficient c_b, is essential for a successful working device.

It is known [6] that spin speed ω, moment of inertia I, and support damping C, all influence the stability of balanced operation. This dependence will be investigated in future studies, where we invisage using numerical continuation, to compute bifurcation diagrams showing the boundaries of stability in various parameter planes [5].

References

[1] Lee J. and Van Moorhem W. K., Analytical and experimental analysis of a self compensating dynamic balancer in a rotating mechanism, *ASME Journal of Dynamic Systems, Measurement and Control* **118** (1996) 468-475.

[2] Thearle E., A new type of dynamic-balancing machine, *Trans. ASME* **54**(APM-54-12) (1932) 131-141.

[3] Chung J. Jang I., Dynamic response and stability analysis of an automatic ball balancer for a flexible rotor. *Journal of Sound and Vibration* **259**(1) (2003) 31-43.

[4] Chao C.-P. Huang Y.-D. Sung C.-K., Non-planar dynamic modeling for the optical disk drive spindles equipped with an automatic balancer. *Mechanism and Machine Theory* **38** (2003) 1289-1305.

[5] Green K. Champneys A. R. and Lieven N. J., Bifurcation analysis of an automatic dynamic balancer for eccentric rotors. *Journal of Sound and Vibration* **291** (2006) 861-881.

[6] Sperling L. Ryzhik B. Linz Ch. and Duckstein H., Simulation of two-plane automatic balancing of a rigid rotor, *Mathematics and computers in simulation* **58** (2002) 351-365.

[7] Genta G. Delprete C. and Busa E., Some considerations on the basic assumptions in rotordynamics, *Journal of Sound and Vibration* **227**(3) (1999) 611-645.

APPENDIX

The explicit forms for the kinetic energy $\mathcal{T}$, potential $\mathcal{V}$ and Rayleigh's dissapation function $\mathcal{F}$ which are derived in Section 2 are given here

$$\begin{aligned}
\mathcal{T} = {} & \frac{1}{2}I_x\left(\dot{\phi}\cos\theta\cos\psi+\dot{\theta}\sin\psi\right)^2+\frac{1}{2}I_y\left(-\dot{\phi}\cos\theta\sin\psi+\dot{\theta}\cos\psi\right)^2+\frac{1}{2}I_z\left(\dot{\phi}\sin\theta+\dot{\psi}\right)^2 \\
& +\frac{1}{2}M\left(\dot{X}^2+\dot{Y}^2+\dot{Z}^2\right) \\
& \frac{1}{2}\sum_{i=1}^{2n+2}m_i\Big\{\Big[\dot{X}+\varepsilon_i\Big(-\sin\theta\dot{\theta}\cos\left(\psi+\alpha_i\right)-\cos\theta\sin\left(\psi+\alpha_i\right)\left(\dot{\psi}+\dot{\alpha}_i\right)\Big)+z_i\cos\theta\dot{\theta}\Big]^2 \\
& +\Big[\dot{Y}+\varepsilon_i\Big(\cos\theta\dot{\theta}\sin\phi\cos\left(\psi+\alpha_i\right)+\sin\theta\cos\phi\dot{\phi}\cos\left(\psi+\alpha_i\right) \\
& \quad -\sin\theta\sin\phi\sin\left(\psi+\alpha_i\right)\left(\dot{\psi}+\dot{\alpha}_i\right)-\sin\phi\dot{\phi}\sin\left(\psi+\alpha_i\right) \\
& \quad +\cos\phi\cos\left(\psi+\alpha_i\right)\left(\dot{\psi}+\dot{\alpha}_i\right)\Big)+z_i\Big(\sin\theta\dot{\theta}\sin\phi-\cos\theta\cos\phi\dot{\phi}\Big)\Big]^2 \\
& +\Big[\dot{Z}+\varepsilon_i\Big(-\cos\theta\dot{\theta}\cos\phi\cos\left(\psi+\alpha_i\right)+\sin\theta\sin\phi\dot{\phi}\cos\left(\psi+\alpha_i\right) \\
& \quad +\sin\theta\cos\phi\sin\left(\psi+\alpha_i\right)\left(\dot{\psi}+\dot{\alpha}_i\right)+\cos\phi\dot{\phi}\sin\left(\psi+\alpha_i\right) \\
& \quad +\sin\phi\cos\left(\psi+\alpha_i\right)\left(\dot{\psi}+\dot{\alpha}_i\right)\Big)+z_i\Big(-\sin\theta\dot{\theta}\cos\phi-\cos\theta\sin\phi\dot{\phi}\Big)\Big]^2\Big\}, \qquad \text{(A-1)}
\end{aligned}$$

$$\mathcal{V}=\frac{1}{2}\sum_{j=1}^{2}\left\{k_{x_j}\left(X+\sin\theta\,\tilde{l}_j\right)^2+k_{y_j}\left(Y-\cos\theta\sin\phi\,\tilde{l}_j\right)^2+k_{z_j}\left(Z-\left(1-\cos\theta\cos\phi\right)\tilde{l}_j\right)^2\right\}, \qquad \text{(A-2)}$$

$$\begin{aligned}
\mathcal{F} = {} & \frac{1}{2}\sum_{j=1}^{2}\Big\{c_{x_j}\left(\dot{X}+\cos\theta\dot{\theta}\,\tilde{l}_j\right)^2+c_{y_j}\left(\dot{Y}+\left(\sin\theta\dot{\theta}\sin\phi-\cos\theta\cos\phi\dot{\phi}\right)\tilde{l}_j\right)^2 \\
& c_{z_j}\left(\dot{Z}-\left(\sin\theta\dot{\theta}\cos\phi+\cos\theta\sin\phi\dot{\phi}\right)\tilde{l}_j\right)^2\Big\}+\frac{1}{2}\sum_{i=3}^{2n+2}c_b\dot{\alpha}_i. \qquad \text{(A-3)}
\end{aligned}$$